

Instability of Reissner-Nordström black hole in Einstein-Maxwell-scalar theory

Yun Soo Myung^{a*} and De-Cheng Zou^{a,b†}

^aInstitute of Basic Sciences and Department of Computer Simulation, Inje University
Gimhae 50834, Korea

^bCenter for Gravitation and Cosmology and College of Physical Science and Technology,
Yangzhou University, Yangzhou 225009, China

Abstract

The scalarization of Reissner-Nordström black holes was recently proposed in the Einstein-Maxwell-scalar theory. Here, we show that the appearance of the scalarized Reissner-Nordström black hole is closely related to the Gregory-Laflamme instability of the Reissner-Nordström black hole without scalar hair.

*e-mail address: ysmyung@inje.ac.kr

†e-mail address: dczou@yzu.edu.cn

1 Introduction

Recently, the scalarized black hole solutions were found from Einstein-scalar-Gauss-Bonnet (ESGB) theories [1, 2, 3]. We note that these black holes with scalar hair are connected to the appearance of instability for the Schwarzschild black hole without scalar hair. Interestingly, the instability of Schwarzschild black hole in ESGB theory is regarded as not the tachyonic instability but the Gregory-Laflamme (GL) instability [4] by comparing it with the instability of the Schwarzschild black hole in the Einstein-Weyl gravity [5].

The notion of the GL instability comes from the three observations [6, 7, 8, 9]: i) The instability is based on the $s(l=0)$ -mode perturbations for scalar and tensor fields. ii) The linearized equation includes an effective mass term, providing that the potential develops negative region near the black hole horizon but it becomes positive after crossing the r -axis. iii) The instability of a black hole without hair is closely related to the appearance of a newly black hole with hair.

More recently, a scalarization of the Reissner-Nordström (RN) black hole was proposed in the Einstein-Maxwell-scalar (EMS) theory which is considered as a simpler theory than the ESGB theory [10]. The EMS theory includes three physically propagating modes of scalar, vector, and tensor. In this case, the instability of RN black hole is determined solely by the linearized scalar equation because the RN black hole is stable against tensor-vector perturbations, as found in the Einstein-Maxwell theory [11, 12, 13, 14]. In this work, we wish to show that the appearance of the scalarized RN black hole is closely associated with the GL instability of the RN black hole without scalar hair.

The organization of our work is as follows. We introduce the EMS theory and its linearized theory around the RN black hole background in section 2. In section 3, we perform the stability analysis for the RN black hole by making use of the linearized scalar equation (18). Mainly, we derive the GL instability bound (20). We solve the static scalar equation (21) to confirm the threshold of the instability α_{th} in section 5. In section 6, we obtain a scalarized RN black hole by solving the four equations (27)-(30) numerically. It indicates that the appearance of the scalarized RN black hole is closely related to the GL instability of the RN black hole without scalar hair. Finally, we discuss our main results in section 6.

2 EMS and its linearized theory

The EMS theory is given by [10]

$$S_{\text{EMS}} = \frac{1}{16\pi} \int d^4x \sqrt{-g} \left[R - 2\partial_\mu\phi\partial^\mu\phi - V_\phi - e^{\alpha\phi^2} F^2 \right], \quad (1)$$

where ϕ is the scalar field with a potential V_ϕ , α is a positive coupling constant, and $F^2 = F_{\mu\nu}F^{\mu\nu}$ is the Maxwell kinetic term. Here we choose $V_\phi = 0$ for simplicity. This theory implies that three of scalar, vector, and tensor are physically dynamical fields. It is noted that a different coupling of $e^{-2\alpha_0\phi}$ was introduced for the Einstein-Maxwell-dilaton theory originating from a low-energy limit of string theory [15, 16].

Now, let us derive the Einstein equation from the action (1)

$$G_{\mu\nu} = 2\partial_\mu\phi\partial_\nu\phi - (\partial\phi)^2 g_{\mu\nu} + 2e^{\alpha\phi^2} T_{\mu\nu}, \quad (2)$$

where $G_{\mu\nu} = R_{\mu\nu} - (R/2)g_{\mu\nu}$ is the Einstein tensor and $T_{\mu\nu} = F_{\mu\rho}F_\nu^\rho - F^2 g_{\mu\nu}/4$ is the Maxwell energy-momentum tensor. The Maxwell equation is given by

$$\nabla^\mu F_{\mu\nu} - 2\alpha\phi\nabla^\mu(\phi)F_{\mu\nu} = 0. \quad (3)$$

The scalar equation takes the form

$$\square\phi - \frac{\alpha}{2}e^{\alpha\phi^2} F^2\phi = 0. \quad (4)$$

Considering $\bar{\phi} = 0$ and electrically charged $\bar{A}_t = Q/r$, one finds the RN solution from (2) and (3)

$$ds_{\text{RN}}^2 = \bar{g}_{\mu\nu}dx^\mu dx^\nu = -f(r)dt^2 + \frac{dr^2}{f(r)} + r^2 d\Omega_2^2 \quad (5)$$

with the metric function

$$f(r) = 1 - \frac{2M}{r} + \frac{Q^2}{r^2}. \quad (6)$$

Here, the outer horizon is located at $r = r_+ = M + \sqrt{M^2 - Q^2}$, while the inner horizon is at $r = r_- = M - \sqrt{M^2 - Q^2}$. It is worth noting that (5) dictates a charged black hole solution without scalar hair.

In order to explore the stability analysis, one has to obtain the linearized theory which describes the metric perturbation $h_{\mu\nu}$, vector perturbation a_μ and scalar perturbation φ

propagating around the RN background (5). By linearizing (2), (3), and (4), we find three linearized equations as

$$\delta G_{\mu\nu}(h) = 2\delta T_{\mu\nu}, \quad (7)$$

$$\bar{\nabla}^\mu f_{\mu\nu} = 0, \quad (8)$$

$$\left(\bar{\square} + \alpha \frac{Q^2}{r^4}\right)\varphi = 0, \quad (9)$$

where the linearized Einstein tensor $\delta G_{\mu\nu}$, the linearized energy-momentum tensor $\delta T_{\mu\nu}$, and the linearized Maxwell tensor $f_{\mu\nu}$ are given by

$$\delta G_{\mu\nu} = \delta R_{\mu\nu} - \frac{1}{2}\bar{g}_{\mu\nu}\delta R - \frac{1}{2}\bar{R}h_{\mu\nu}, \quad (10)$$

$$\begin{aligned} \delta T_{\mu\nu} &= \bar{F}_\nu{}^\rho f_{\mu\rho} + \bar{F}_\mu{}^\rho f_{\nu\rho} - \bar{F}_{\mu\rho}\bar{F}_{\nu\sigma}h^{\rho\sigma} \\ &+ \frac{1}{2}(\bar{F}_{\kappa\eta}f^{\kappa\eta} - \bar{F}_{\kappa\eta}\bar{F}^\kappa{}_\sigma h^{\eta\sigma})\bar{g}_{\mu\nu} - \frac{1}{4}\bar{F}^2 h_{\mu\nu}, \end{aligned} \quad (11)$$

$$f_{\mu\nu} = \partial_\mu a_\nu - \partial_\nu a_\mu. \quad (12)$$

We note that an effective mass term of $\alpha Q^2/r^4$ in (9) is replaced by $2\lambda^2 M^2/r^6$ in the ESGB theory [5]. Here ‘ α ’ plays the role of a mass-like parameter. However, it seems that the effective mass $\mu_{\text{eff}}^2 = -\alpha Q^2/r^2 < 0$ in Ref.[10] is not a correct expression.

3 Instability of RN black hole

In analyzing the stability of the RN black hole in the EMS theory, we first consider the two linearized equations (7) and (8) because two perturbations of metric $h_{\mu\nu}$ and vector a_μ are coupled. Exactly, these correspond to the linearized equations for the Einstein-Maxwell theory. For the odd-parity perturbations, one found the Zerilli-Moncrief equation which describes two physical DOF propagating around the RN black hole background [11, 12]. Also, the even-parity perturbations with two physical degrees of freedom (DOF) were studies in [13, 14]. It turns out that the RN black hole is stable against these perturbations. In this case, a massless spin-2 mode starts with $l = 2$, while a massless spin-1 mode begins with $l = 1$. The EMS theory provides 5(=2+2+1) DOF propagating around the RN background.

Now, we focus on the linearized scalar equation (9) which determines the stability of the RN black hole critically in the EMS theory. Introducing

$$\varphi(t, r, \theta, \varphi) = \frac{u(r)}{r}e^{-i\omega t}Y_{lm}(\theta, \varphi), \quad (13)$$

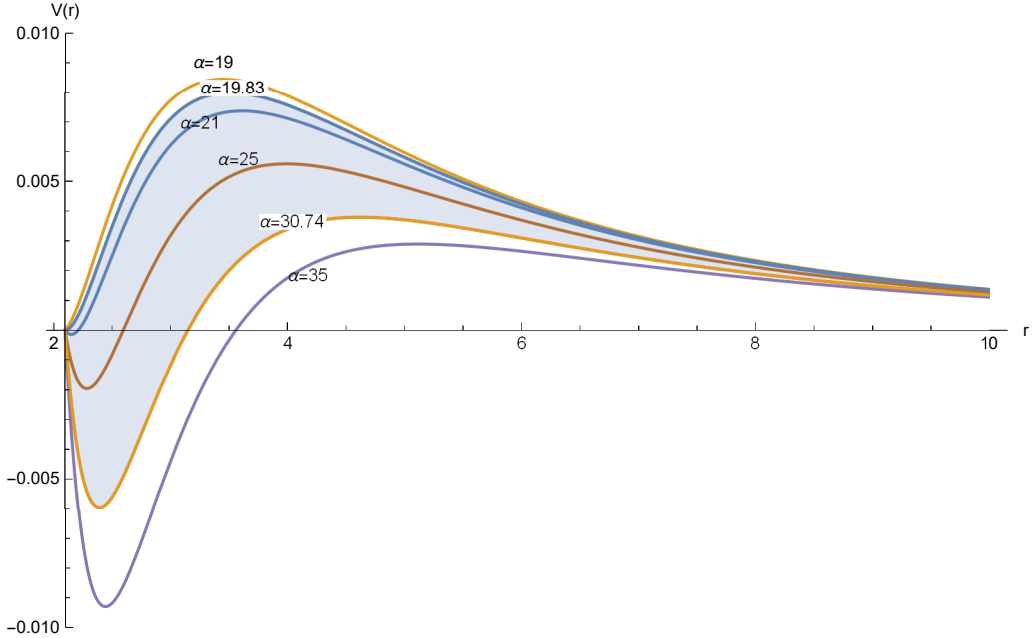


Figure 1: The α -dependent potentials as function of $r \in [r_+, \infty)$ for the outer horizon radius $r_+ = 2.09$ ($q = Q/M = 0.418$) and $l = 0$. From the top, each curve represents the potential $V(r)$ of a scalar field for the parameter $\alpha = 19$ (stable), 19.83 (positive definite potential), 21, 25, 30.74 (sufficient condition for instability), and 35 (unstable case), respectively. The potentials have negative regions near the outer horizon for $\alpha > 19.83$. One conjectures that the threshold of GL instability is located at α between $\alpha = 19.83$ and $\alpha = 30.74$ (shaded region).

and considering a tortoise coordinate r_* defined by $dr_* = dr/f(r)$, a radial equation of (9) leads to the Schrödinger-type equation

$$\frac{d^2u}{dr_*^2} + [\omega^2 - V(r)]u(r) = 0, \quad (14)$$

where the scalar potential $V(r)$ is given by

$$V(r) = f(r) \left[\frac{2M}{r^3} + \frac{l(l+1)}{r^2} - \frac{2Q^2}{r^4} - \alpha \frac{Q^2}{r^4} \right]. \quad (15)$$

In Fig. 1, we find the α -dependent potentials for given $l = 0$, $M = 1.1$ and $Q = 0.46$ (a non-extremal RN black hole). The $s(l = 0)$ -mode is allowed for the scalar perturbation and it is regarded as an important mode to test the stability of the RN black hole. Hereafter, thus, we consider this mode only. A sufficient condition of $\int_{r_+}^{\infty} dr V(r)/f(r) < 0$ for instability

leads to the bound as

$$\alpha > \alpha_{\text{in}}(q) \equiv \frac{3 - 2q^2 + 3\sqrt{1 - q^2}}{q^2} \quad (16)$$

with $q = Q/M$. The first term of $3/q^2$ was found in analyzing the black hole dynamics in Einstein-Maxwell-dilaton theory [15]. On the other hand, by observing the potential (15) carefully, the positive definite potential without negative region near the horizon could be implemented by imposing the bound

$$\alpha \leq \alpha_{\text{po}}(q) \equiv \frac{2\sqrt{1 - q^2}(1 + \sqrt{1 - q^2})}{q^2}, \quad (17)$$

which guarantees the stable RN black hole. In the extremal limit of $q \rightarrow 1$, one finds that $\alpha_{\text{th}} \rightarrow 1$ and $\alpha_{\text{po}} \rightarrow 0$. We note that (16) is not a necessary and sufficient condition for the instability. Observing Fig. 1 together with $q = 0.418$, one finds that two potential curves with $\alpha = 21, 25$ between $\alpha_{\text{po}} = 19.83 < \alpha < \alpha_{\text{in}} = 30.7$ develop negative regions near the horizon but they become positive after crossing the r -axis.

At this stage, we would like to mention that such potentials exist around neutral black holes (black holes without charge) in higher dimensions and the S-deformation has been used to confirm the stability of neutral black holes in higher dimensions [17]. We conjecture that the GL instability may occur in the shaded region between $19.83 < \alpha_{\text{th}} < 30.74$, but the threshold of instability α_{th} should be determined explicitly by the numerical computations. Usually, if the potential V derived from physically propagating modes is negative in some region, a growing perturbation can appear in the spectrum. This might indicate an instability of the black hole system under such perturbations. However, this is not always true. Some potentials with negative region near the horizon still do not imply the instability. The criterion to determine whether a black hole is stable or not against the perturbation is whether the time-evolution of the perturbation is decaying or not. The perturbed equation around a RN black hole can usually be described by the Schrödinger-type equation, where a growing mode like $e^{\Omega t}$ of the perturbation indicates the instability of the black hole. The absence of any unstable modes based on physical fields provides a precise way of determining the stability of the black hole. Here, even though the RN black hole is unstable for $\alpha > \alpha_{\text{th}} = 29.74$, it is stable for $19.83 < \alpha < 29.74$ giving negative region near the horizon. In this sense, the S-deformation seems not to be a correct way to establish the stability of such black holes.

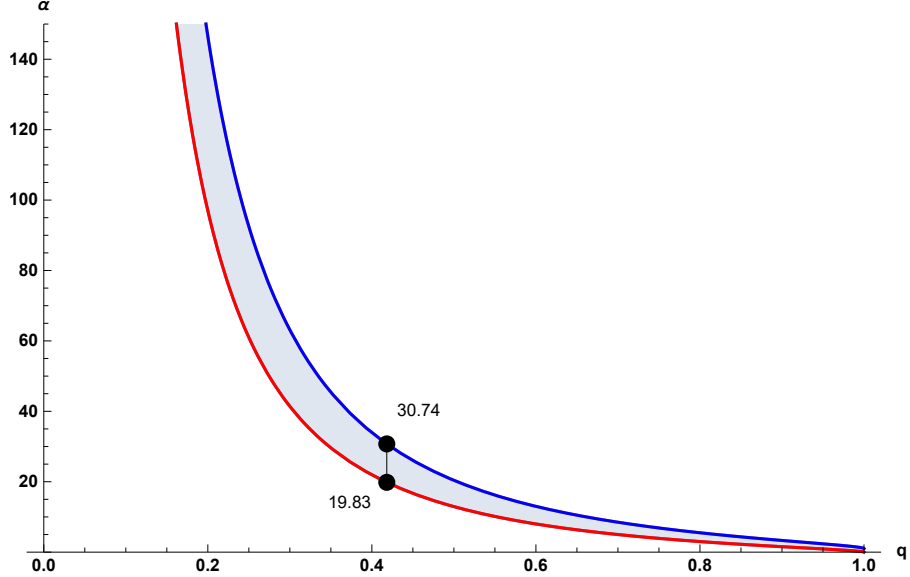


Figure 2: Two α -curves as function of $q \in (0, 1]$ and its shaded region between them. The upper curve represents $\alpha_{\text{in}}(q)$ in (16), while the lower one denotes $\alpha_{\text{po}}(q)$ in (17). For $q = 0.418$, they correspond to $\alpha_{\text{in}} = 30.74$ and $\alpha_{\text{po}} = 19.83$.

From Fig. 2 depicting α_{in} (16) and α_{po} (17), we expect that the threshold of an $s(l=0)$ -mode instability is located at the shaded region between α_{in} and α_{po} . Two curves go apart as $q \rightarrow 0$ (Schwarzschild black hole), while they approach each other as $q \rightarrow 1$ (extremal black hole).

To determine the threshold of instability explicitly, one has to solve the second-order differential equation numerically

$$\frac{d^2u}{dr_*^2} - [\Omega^2 + V(r)]u(r) = 0, \quad (18)$$

which allows an exponentially growing mode of $e^{\Omega t}(\omega = i\Omega)$ as an unstable mode. Here we choose two boundary conditions: a normalizable solution of $u(\infty) \sim e^{-\Omega r_*}$ at infinity and a solution of $u(r_+) \sim (r - r_+)^{\Omega r_+}$ near the outer horizon. Observing Fig. 3, we read off the threshold of instability $\alpha_{\text{th}}(q) = \{88.98, 60.69, 29.47, 15.46, 8.019, 2.995\}$ at $q = \{0.25, 0.3, 0.418, 0.55, 0.7, 0.9\}$. From Fig. 4, also, one finds that the threshold of instability is between the sufficient condition for instability $\alpha_{\text{in}}(q) \approx \{92.48, 63.13, 30.74, 16.2, 8.45, 3.318\}$ and the condition for positive definite potential $\alpha_{\text{po}}(q) \approx \{68.98, 41.42, 19.85, 10.13, 4.997, 1.545\}$

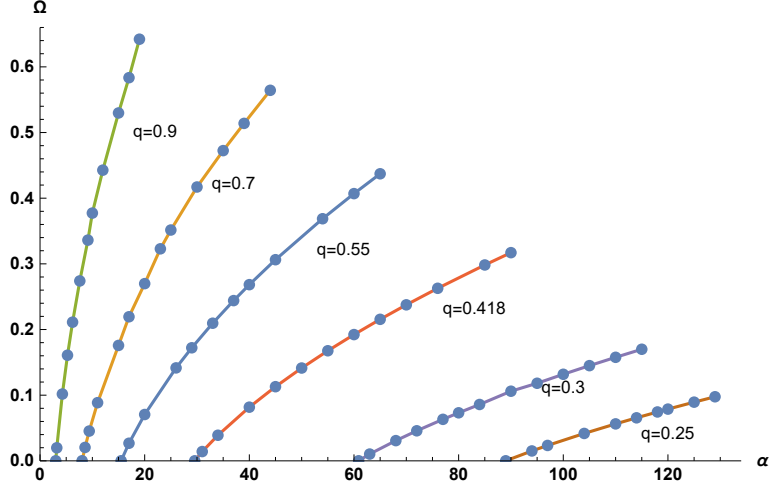


Figure 3: Plots of unstable modes (\bullet) on six different curves with $q = \{0.25, 0.3, 0.418, 0.55, 0.7, 0.9\}$. The $y(x)$ -axis denote Ω in $e^{\Omega t}$ (mass-like parameter α of scalar mode). Here we observe that the thresholds of instability are located at $\alpha_{\text{th}}(q) \approx \{88.98, 60.69, 29.47, 15.46, 8.019, 2.995\}$.

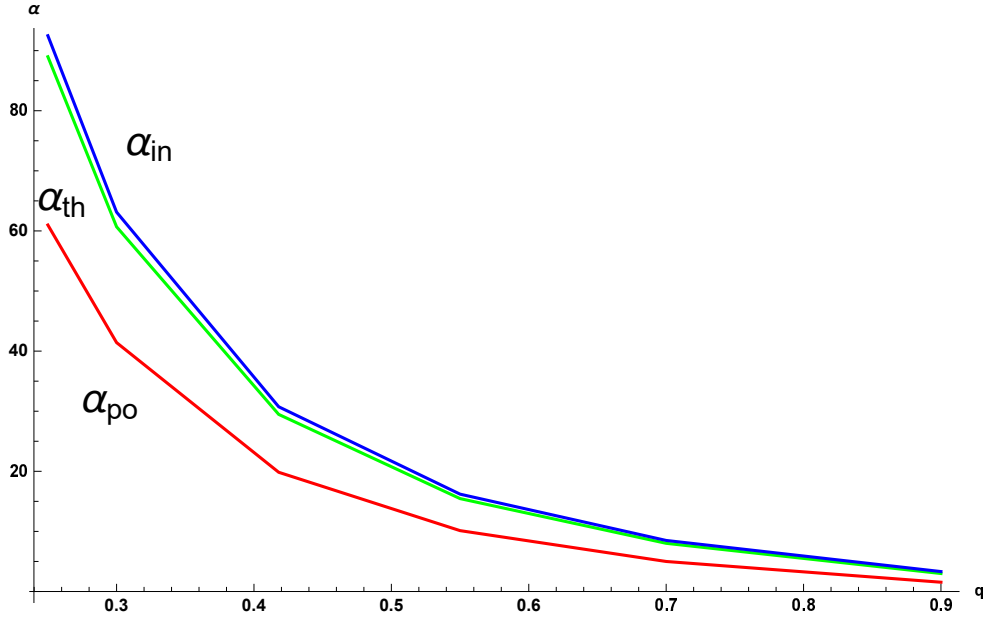


Figure 4: Three α -curves as function of q . The upper blue curve represents $\alpha_{\text{in}}(q)$ in (16) and the middle green curve indicates $\alpha_{\text{th}}(q)$, while the lower red one denotes $\alpha_{\text{po}}(q)$ (17). We find an inequality of $\alpha_{\text{po}}(q) < \alpha_{\text{th}}(q) < \alpha_{\text{in}}(q)$.

at $q = \{\dots\}$. This proves that an inequality is satisfied as

$$\alpha_{\text{po}}(q) < \alpha_{\text{th}}(q) < \alpha_{\text{in}}(q), \quad (19)$$

where $\alpha_{\text{po}}(q)$ and $\alpha_{\text{in}}(q)$ are given by (17) and (16), while $\alpha_{\text{th}}(q)$ is determined by solving (18) numerically.

Consequently, the instability bound for the RN black hole is given by

$$\alpha > \alpha_{\text{th}}(q) \quad (20)$$

which is considered as one of our main results. However, we could not determine an explicit form of $\alpha_{\text{th}}(q)$ as function of q like as $\alpha_{\text{in}}(q)$ in (16).

4 $\omega = 0$ scalar perturbation

Here, it is worth checking the instability bound (20) of the RN black hole again, especially for finding $\alpha_{\text{th}}(q)$. This can be achieved by obtaining the static scalar solutions to the linearized equation (14) with $\omega = 0$ on the background of the RN black hole. For a given $l = 0$ and q , requiring an asymptotically vanishing lead to the fact that the presence of a smooth scalar determines a discrete set for α . The bifurcation requires α above a minimal value α_{min} .

Introducing a static condition ($\omega = 0$) and a new coordinate of $z = r/2M$, the equation for $u(r)$ reduces to

$$f(z)u''(z) + f'(z)u'(z) - \left(\frac{\alpha q^2}{4z^4} - \frac{f'(z)}{z} \right) u(z) = 0, \quad (21)$$

where $f(z) = (z - z_-)(z - z_+)/z^2$ with $z_{\pm} = (1 \pm \sqrt{1 - q^2})/2$.

One has to find a numerical solution because any analytic solution is not available. For this purpose, we first propose the near-horizon expansion for $u(z)$ as

$$u(z) = u_+ + u'_+(z - z_+) + \frac{u''_+}{2}(z - z_+)^2 + \dots \quad (22)$$

This expression can be used to set data outside the outer horizon for a numerical integration from $z = z_+$ to $z = \infty$. Here the coefficients u'_+ and u''_+ could be determined in terms of a free parameter u_+ as

$$u'_+ = -\frac{\alpha q^2 + 4z_+(z_- - z_+)}{4z_+^2(z_+ - z_-)}u_+, \quad u''_+ = \frac{\alpha q^2(\alpha q^2 + 8z_- z_+)}{32z_+^4(z_+ - z_-)^2}u_+. \quad (23)$$

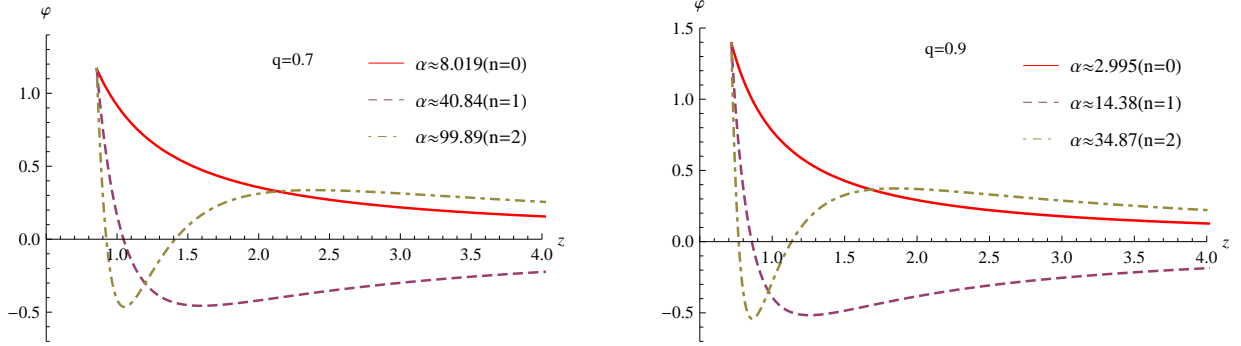


Figure 5: Radial profiles of φ as function of $z = r/(2M)$ for the first three perturbed scalarized solutions. The left-handed picture is depicted for $q = 0.7$, while the right-handed one is designed for $q = 0.9$ (near-extremal black hole).

An asymptotic form of $u(z)$ near the infinity of $z = \infty$ is given by

$$u(z) = u_\infty + \frac{u^{(1)}}{z} + \frac{u^{(2)}}{z^2} + \dots, \quad (24)$$

where two relations are expressed in terms of u_∞ as

$$u^{(1)} = \frac{z_- + z_+}{2} u_\infty, \quad u^{(2)} = \frac{-\alpha q^2 + 8(z_-^2 + z_- z_+ + z_+^2)}{24} u_\infty. \quad (25)$$

At this stage, we perform two integrations: from $z = z_+$ to a matching point $z = z_m > z_+$ by imposing the ingoing wave boundary condition at the outer horizon and from $z = \infty$ to $z = z_m$ by requiring no outgoing wave at infinity. Then, a numerical solution could be obtained by connecting the near-horizon form (22) to the asymptotic form (24) together with selecting the parameter α : $\alpha_n(q = 0.7) \approx \{8.019, 40.84, 99.89, \dots\}$ and $\alpha_n(q = 0.9) \approx \{2.995, 14.38, 34.87, \dots\}$. The other four spectra are given by $\alpha_n(0.55) \approx \{15.46, 80.02, 196.1, \dots\}$, $\alpha_n(0.418) \approx \{29.47, 153.9, 377.7, \dots\}$, $\alpha_n(0.3) \approx \{60.69, 318.4, 382.0, \dots\}$, and $\alpha_n(0.25) \approx \{88.98, 467.43, 1148, \dots\}$. In Fig. 5, these solutions are classified by the order number $n = 0, 1, 2, \dots$ which is identified with the number of nodes for $\varphi(z) = u(z)/z$. We find that the $n = 0$ scalar mode without zero crossing represents the edge of the domain of instability, while the $n = 1$ and 2 scalar modes with zero crossings denote unstable black holes. This indicates that one may classify charged black holes into unstable and stable black holes by solving the

static linearized scalar equation (21) directly without taking into account an exponentially growing mode of $e^{\Omega t}$. Actually, this corresponds to finding the $l = 0$ bifurcation points from the RN black hole with $q = Q/M$. Finally, we confirm that for given q , $\alpha_{n=0}(q) = \alpha_{\min}(q)$ [underline value] recovers the threshold of instability $\alpha_{\text{th}}(q)$ exactly.

5 Scalarized RN black hole

Before we proceed, we note that the RN black hole solution is allowed for any value of α , while a scalarized RN black hole solution may exist when α satisfies the instability bound (20). The threshold of instability for a RN black hole reflects the disappearance of zero crossings in the perturbed scalar profiles. One expects a close connection between the instability of a RN black hole without scalar hair and appearance of a scalarized RN black hole. As a concrete example, we wish to find a scalarized RN black hole which is closely related to the $q = 0.7$ ($M = 1$, $Q = 0.7$) and $\alpha = 8.019$ case ($n = 0$ case).

For this purpose, let us introduce the metric ansatz as [10]

$$ds_{\text{SRN}}^2 = -N(r)e^{-2\delta(r)}dt^2 + \frac{dr^2}{N(r)} + r^2(d\theta^2 + \sin^2\theta d\varphi^2), \quad (26)$$

where a metric function is defined by $N(r) = 1 - 2m(r)/r$ with the mass function $m(r)$. Also, we consider the $U(1)$ potential and the scalar as $A = V(r)dt$ and $\phi(r)$. Substituting these into Eqs.(2)-(4) leads to the four equations

$$-2m'(r) + e^{2\delta(r)+\alpha\phi(r)^2}r^2V'(r)^2 + [r^2 - 2rm(r)]\phi'(r)^2 = 0, \quad (27)$$

$$\delta'(r) + r\phi'(r)^2 = 0, \quad (28)$$

$$V'(r) + e^{-\delta(r)-\alpha\phi(r)^2}\frac{Q}{r^2} = 0, \quad (29)$$

$$\begin{aligned} & e^{2\delta(r)+\alpha\phi(r)^2}r^2\alpha\phi(r)V'(r)^2 + r[r - 2m(r)]\phi''(r) \\ & - \left(m(r)[2 - 2r\delta'(r)] + r[-2 + r + 2m'(r)]\delta'(r) \right) \phi'(r) = 0. \end{aligned} \quad (30)$$

Assuming the existence of a horizon located at $r = r_+$, one finds an approximate solution

to equations in the near-horizon

$$m(r) = \frac{r_+}{2} + m_1(r - r_+) + \dots, \quad (31)$$

$$\delta(r) = \delta_0 + \delta_1(r - r_+) + \dots, \quad (32)$$

$$\phi(r) = \phi_0 + \phi_1(r - r_+) + \dots, \quad (33)$$

$$V(r) = v_1(r - r_+) + \dots, \quad (34)$$

where the four coefficients are given by

$$m_1 = \frac{e^{-\alpha\phi_0^2}Q^2}{2r_+^2}, \quad \delta_1 = -r_+\phi_1^2, \quad \phi_1 = \frac{\alpha\phi_0Q^2}{r_+(Q^2 - e^{\alpha\phi_0^2}r_+^2)}, \quad v_1 = -\frac{e^{-\delta_0-\alpha\phi_0^2}Q}{r_+^2}. \quad (35)$$

This approximate solution involves two crucial parameters of $\phi_0 = \phi(r_+)$ and $\delta_0 = \delta(r_+)$, which will be found by matching the above expansions (31)-(34) with the asymptotic solutions in the far region

$$\begin{aligned} m(r) &= M - \frac{Q^2 + Q_s^2}{2r} + \dots, \quad \phi(r) = \phi_\infty + \frac{Q_s}{r} + \dots, \\ \delta(r) &= \frac{Q_s^2}{2r^2} + \dots, \quad V(r) = \Phi + \frac{Q}{r} + \dots, \end{aligned} \quad (36)$$

where Q_s and Φ denote the scalar charge and the electrostatic potential, in addition to the ADM mass M and the electric charge Q . For simplicity, we choose $\phi_\infty = 0$ here.

The EMS theory admits the RN black hole solution without scalar hair for any α . However, it becomes an unstable black hole for $\alpha > \alpha_{\text{th}}(q)$ (20), while it is stable against the scalar perturbation for $\alpha < \alpha_{\text{th}}(q)$. We note that “ $\alpha = \alpha_{\text{th}}(q)$ ” indicates the threshold of instability. One expects that a scalarized RN black hole is allowed for $\alpha \geq \alpha_{\text{th}}(q)$ when $q \geq 0.7$. This means that the scalarized RN black holes bifurcates from the RN black hole for $\alpha \geq \alpha_{\text{th}}(q)$, but q increases beyond unity for the fixed α , implying that the scalarized RN black hole could be overcharged.

For the RN black hole with $\phi_0 = 0$, the outer horizon is located at $r_+ = 1.714$ and the charge-mass ratio is given by $q = 0.7$. They are starting points for existing a scalarized RN black hole. In the Fig.6 (left), one observes that for given $\alpha = 8.019$, the ratio of q for the scalarized RN black hole increases beyond the maximum ratio $q = 1$ for the RN black hole as ϕ_0 increases. This means that the scalar at the horizon ϕ_0 is allowed only for $q \geq 0.7$. Moreover, in the Fig. 6 (right), the scalar at the horizon ϕ_0 increases as the horizon radius r_+ of the scalarized RN black hole decreases. The scalar at the horizon is

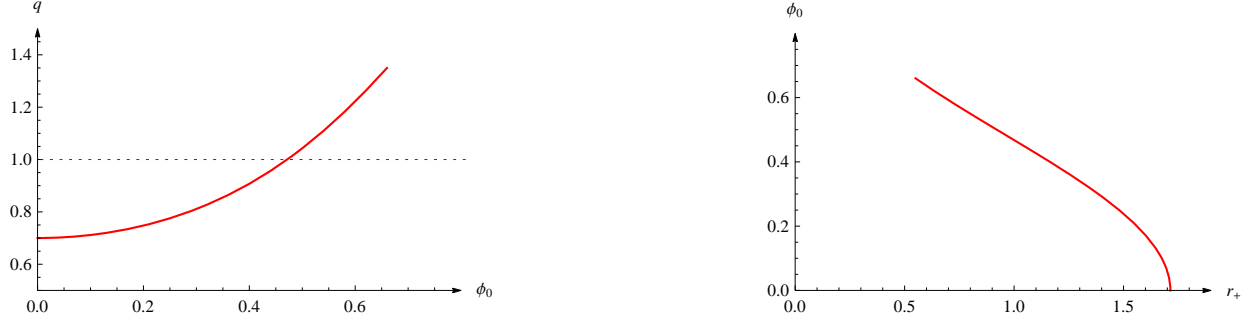


Figure 6: (left) The charge-mass ratio q for the scalarized RN black hole as a function of ϕ_0 with the fixed $\alpha = 8.019$. The dotted horizontal line represents the maximum ratio $q = 1$ for the RN black hole. (right) The scalar at the horizon ϕ_0 as a function of the horizon radius r_+ for the scalarized black hole. This corresponds to the $n = 0$ case.

terminated at $r_+ = 1.714$, corresponding to the RN outer horizon. As shown in Fig. 1 of Ref. [10], the scalarized RN black hole emerges when $q \geq 0.7$ in the case of the fixed $\alpha = 8.019$. In addition, it is true that there exists a constraint of $0 < q \leq 1$ for the RN black hole. However, this is broken for the scalarized RN black hole, implying that the ratio q becomes larger than 1 for $\phi_0 > 0.47$.

It is known that the scalarization bands exist for the ESGB theory [3]. A discrete set for η/M^2 obtained from static scalar perturbation corresponds to the right-end values of scalarization bands for a scalarized Schwarzschild black hole, while the left-end values are provided by the regularity constraint at the horizon ($r_+^4 - 6\eta^2\phi_0^2 \geq 0$). However, as is shown in Fig. 7, there are no scalarization bands in the EMS theory because we do not need to impose the regularity condition at the horizon. As a result, there is no upper bound on α to each $n = 0, 1, 2$.

Consequently, we obtain the scalarized RN black hole solution depicted in Fig. 8. This corresponds to one of our main results. The metric function $N(r)$ has a different horizon at $\ln r = \ln r_+ = 0.067$ in compared to the RN horizon at $\ln r = \ln r_+ = 0.539$ and it approaches the RN metric function $f(r)$ as $\ln r$ increases. Also, the scalar hair $\phi(r)$ starts with $\phi_0 = 0.44$ at the horizon and it decreases as $\ln r$ increases, in compared to $\phi(r) = 0$ for the RN black hole.

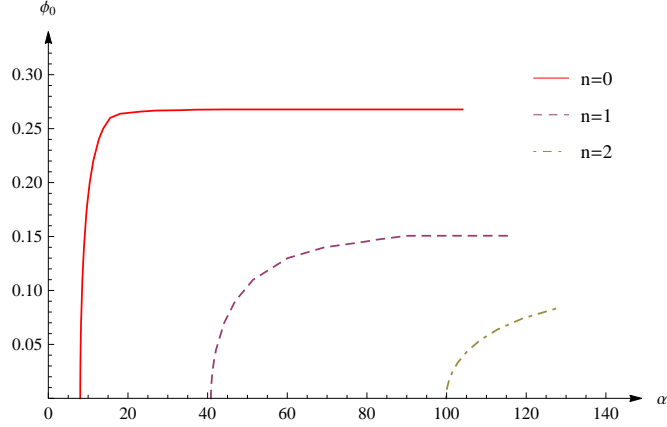


Figure 7: The scalar field $\phi_0 = \phi(r_+)$ at the horizon as a function of mass-like parameter α . All the nontrivial branches with $n = 0, 1, 2$ start from bifurcation points at $\alpha_n = \{8.019, 40.84, 99.89\}$ on the trivial branch (RN black holes on α -axis). They span whole region without bound.

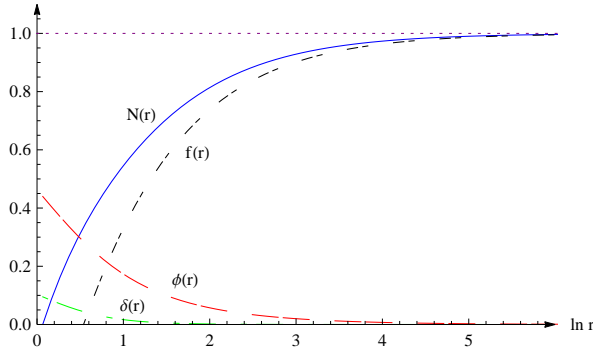


Figure 8: The scalarized RN solution for the $n = 0$ case. Two metric functions $f(r)$ for RN and $N(r)$ for scalarized RN as function of r with $\alpha = 8.019$. We observe that the logarithmic values of horizon radius of scalarized RN and RN black holes are located at 0.067 and 0.539, respectively. The scalar hair $\phi(r)$ starts with $\phi_0 = 0.44$ at the horizon and it decreases as $\ln r$ increases.

6 Discussions

First of all, we have derived the GL instability bound (20) for the RN black hole in the EMS theory by considering $s(l = 0)$ -mode scalar perturbation. This bound does not take

an analytic form because as was shown in Fig. 3, it was determined from solving the scalar perturbed equation (9) numerically. On the other hand, an analytic bound is given by (16) which was derived from the sufficient condition for the instability. We have obtained α_{th} again by solving the static scalar perturbed equation numerically. Finally, we have found the scalarized RN black hole for $\alpha = \alpha_{\text{th}} = 8.019$ ($n = 0$ case) and $q \geq 0.7$ by solving Eqs. (27)-(30) numerically. Also, it is worth noting that the scalarized RN black hole is not allowed for $q < 0.7$ ($r_+ > 1.714$) for $\alpha = 8.019$ which corresponds to the stable RN black hole.

Acknowledgments

This work was supported by the National Research Foundation of Korea (NRF) grant funded by the Korea government (MOE) (No. NRF-2017R1A2B4002057).

References

- [1] G. Antoniou, A. Bakopoulos and P. Kanti, Phys. Rev. Lett. **120**, no. 13, 131102 (2018) doi:10.1103/PhysRevLett.120.131102 [arXiv:1711.03390 [hep-th]].
- [2] D. D. Doneva and S. S. Yazadjiev, Phys. Rev. Lett. **120**, no. 13, 131103 (2018) doi:10.1103/PhysRevLett.120.131103 [arXiv:1711.01187 [gr-qc]].
- [3] H. O. Silva, J. Sakstein, L. Gualtieri, T. P. Sotiriou and E. Berti, Phys. Rev. Lett. **120**, no. 13, 131104 (2018) doi:10.1103/PhysRevLett.120.131104 [arXiv:1711.02080 [gr-qc]].
- [4] R. Gregory and R. Laflamme, Phys. Rev. Lett. **70**, 2837 (1993) doi:10.1103/PhysRevLett.70.2837 [hep-th/9301052].
- [5] Y. S. Myung and D. C. Zou, Phys. Rev. D **98**, no. 2, 024030 (2018) doi:10.1103/PhysRevD.98.024030 [arXiv:1805.05023 [gr-qc]].
- [6] B. Whitt, Phys. Rev. D **32**, 379 (1985). doi:10.1103/PhysRevD.32.379
- [7] Y. S. Myung, Phys. Rev. D **88**, no. 2, 024039 (2013) doi:10.1103/PhysRevD.88.024039 [arXiv:1306.3725 [gr-qc]].
- [8] H. L. A. Perkins, C. N. Pope and K. S. Stelle, Phys. Rev. D **96**, no. 4, 046006 (2017) doi:10.1103/PhysRevD.96.046006 [arXiv:1704.05493 [hep-th]].
- [9] K. S. Stelle, Int. J. Mod. Phys. A **32**, no. 09, 1741012 (2017). doi:10.1142/S0217751X17410123
- [10] C. A. R. Herdeiro, E. Radu, N. Sanchis-Gual and J. A. Font, arXiv:1806.05190 [gr-qc].
- [11] F. J. Zerilli, Phys. Rev. D **9**, 860 (1974). doi:10.1103/PhysRevD.9.860
- [12] V. Moncrief, Phys. Rev. D **9**, 2707 (1974). doi:10.1103/PhysRevD.9.2707
- [13] V. Moncrief, Phys. Rev. D **10**, 1057 (1974). doi:10.1103/PhysRevD.10.1057
- [14] V. Moncrief, Phys. Rev. D **12**, 1526 (1975). doi:10.1103/PhysRevD.12.1526
- [15] E. W. Hirschmann, L. Lehner, S. L. Liebling and C. Palenzuela, Phys. Rev. D **97**, no. 6, 064032 (2018) doi:10.1103/PhysRevD.97.064032 [arXiv:1706.09875 [gr-qc]].

- [16] C. Pacilio, arXiv:1806.10238 [gr-qc].
- [17] H. Kodama and A. Ishibashi, Prog. Theor. Phys. **111**, 29 (2004) doi:10.1143/PTP.111.29 [hep-th/0308128].